**Faculty of Natural and Applied Sciences Journal of Scientific Innovations**
**Print ISSN: 2814-0877 e-ISSN: 2814-0923**
www.fnasjournals.com
**Volume 6; Issue 3; May 2025; Page No. 1-14.**
**DOI:** https://doi.org/10.63561/fnas-jsi.v6i3.945

# Multifaceted Investigations of Mixed-Ligand Metal (II) Complexes: Synthesis, Characterization, DFT, and Biological Studies

***[1]Wodi, T.C., & Festus, C.**
[1]Department of Chemistry, Ignatius Ajuru University of Education, Rivers State, Nigeria
[2]Community Boys Senior Secondary, Elelenwo, Port Harcourt, Rivers State, Nigeria.

***Corresponding author email:** chizobawt@gmail.com

**Abstract**
The study described the synthesis, characterization, DFT and biological studies of Mixed-ligand divalent complexes ([M(L1)(L2)]n$H_2O$)(M= $Cu^{2+}$, $Fe^{2+}$ and $Mn^{2+}$, L1=SBL1, L2=SBL2, n=0,I,2,3,4) containing 3-(E)-4-(((2-hydroxynaphthalen-1-yl)methylene)amino)-1,5-dimethyl-2-phenyl-1H-pyrazol-3(2H)-one [SBL1] and (E)-1-(((6-nitrobenzo[d]thiazol-2-yl)imino)methyl)naphthalene-2-ol [SBL2] which were prepared via reflux condensations from their precursors. The ligands, SBL1 and SBL2 were reacted with the acetate (Cu and Mn), and sulphate (Fe) salts in molar ratio of 1:1:1 affording the complexes with various shades of colour distinct from the starting reagents. The melting points of the complexes ranged from 208 to 350$^oC$. The FT-IR spectrum of SBL1 and SBL2 presented a band at 1633$cm^{-1}$ and 1669 $cm^{-1}$ which moved to 1625-1642$cm^{-1}$ in the complexes and was apportioned to an azomethine moiety. The electronic spectra of the [Cu(L1)(L2)], [Fe(L1)(L2)$(H_2O)_2$]$H_2O$, and [Mn(L1)(L2)] are compatible with square planar, tetrahedral, and octahedral geometry. The compounds were found to exhibit one form of action or the other against all the screened microbes with [Mn(L1)(L2)]$H_2O$] displaying the highest inhibitory zone of 15.5mm against *Staphylococcus epidermidis*, which is more effective compared to the positive control (streptomycin).The anti-fungiform study designated that the ligands and its complexes are highly active against *Aspergillums flavus*, *fusarium sp.* and *Aspergillus niger* with SBL2 ligand displaying the highest inhibitory zones of 25.0mm against *Aspergillus niger*.[Cu(L1)(L2)]complex also displayed the highest inhibitory zones of 17mm and 13mm against *Aspergillus niger* and *Aspergillus flavus*. The stereochemistry and electron distribution features of SBL and [M(L1)(L2)]complexes remained examined more by DFT evaluation. The result designated that the SBL and its complexes are soft molecules due to their high tendency of bioavailability and can be a better agent against bacteria. The compounds also showed a high electrophilic value which indicates strong electron acceptor.

**Keywords:** Mixed Ligand, Synthesis, Characterization, Microbial, DFT,

## Introduction
Metal complexes with mixed ligands have garnered significant interest in the field of inorganic chemistry due to their diverse properties and potential applications (Abdullahi et al., 2018; Jean-Pierr & Launay, 2019). These complexes, in which more than one type of ligand is coordinated to the metal centre, exhibit complex geometries, coordination modes, and reactivity patterns that differ from those of single-ligand complexes (Franz & Metzler-nolte, 2019) This versatility makes mixed ligands' metal(II) complexes valuable for various applications, including catalysis, materials science, and bioinorganic chemistry (Farhi et al., 2023; Hema et al., 2024). The synthesis of mixed ligands' metal(II) complexes involves a variety of synthetic methods, including conventional coordination chemistry techniques and advanced organometallic approaches (Farhi et al.,2023; Meena et al., 2022). The selection of ligands and the stoichiometry of the reaction play a crucial role in determining the structure and properties of the resulting complexes (Sandra et al., 2019). Understanding the factors that influence the formation of mixed ligands' metal(II) complexes is key to designing and manipulating their structures for specific applications. The synthesis of mixed ligands' metal(II) complexes involves the coordination of multiple ligands to a metal ion, forming complex structures with distinct


*Cite this article as*:
Wodi, T.C., & Festus, C. (2025). Multifaceted investigations of mixed-ligand metal (II) complexes: synthesis, characterization, DFT, and biological studies. *FNAS Journal of Scientific Innovations*, *6*(3), 1-14. https://doi.org/10.63561/fnas-jsi.v6i3.945

geometries and coordination environments (Franz & Metzler-nolte, 2019). This process requires careful selection of ligands and reaction conditions to control the formation of specific complexes. Synthesis of ligands plays a crucial role in the preparation of mixed ligands' metal(II) complexes. Ligands are organic molecules or ions that coordinate to a central metal ion to form a complex. The selection of ligands and the design of ligand structures are important considerations in the synthesis of such complexes (Festus, 2021). The choice of ligands is a critical factor in determining the properties and behaviour of the resulting metal complex. Previously, we had synthesized few complexes of 2-(thiazole-2-ylamino)-2,3-dihydonaphthalene-1-4-dione Schiff base and studied their corrosion inhibition potentials (Festus & Wodi, 2021). In this paper we present synthesis, characterization, antioxidant, DFT of a mixed-ligand metal complexes with divalent ion Cu, Fe and Mn and biological evaluation of the complexes.

**Materials and Methods**

The chemicals; $C_{11}H_8O_2$, $C_{10}H_60_3$, $C_6H_6ClNO$, $C_7H_5N_3O_2S$, acetate salts (Mn, Cu) sulphate salt (Fe), were purchased from Aldrich Coy Germany. All the reagents were purchased from Aldrich Company Germany and used without further purification. Infrared spectral analysis was determined using Fourier Transform infrared spectrophotometer (FTIR) range 4000-350$cm^{-1}$ ultraviolet and visible spectra measurement was measured using Pekin Elmer Lambda 25uv/Visible Spectrophotometer within the scale 190-400nm and 400-900nm. The antibacterial and antifungal studies were performed exactly as reported by Festus and Wodi (2021). The DFT was carried out for the ligands and mixed ligands metal(II) complexes to the full advancement. Becke 3 lee yan par(Becke, 1992) [BBLYP] in combination with 6-31xG(d.p) set for all atoms excepts for the ions (Mn, Fe, Cu, and Zn) BBlyp/6-31 + G(d,p) + LAN1,2D2 which have been impassively used for M(II) complexes plus has been documented to be appropriate frequency calculation was carried out to determine the nonexistence of imaginary frequencies

**Synthesis of ligands**

Ligands SBL1 and SBL2 were prepared by assimilating ethanolic solution of 2-hydroxyl –1–naphthaldehyde (7.0g, 0.000041mole) and with 20 mL ethanol of 4–amino antipyrine (8.32g, 0.000041mole for SBL1 plus 2-hydroxyl-1,4-naphthoquinone (8.0g, 0.0459mole) 35mL and ethanolic solution of 2-Chloro-4-aminophenol (6.60g, 0.0465mole)30mL for SBL2. Eight (8) drops of acid catalyst was added to mixtures. The resulting solutions were refluxed for 3- 6 hours at 50$^o$c with stirring and then cooled to room temperature. The resulting yellow precipitates formed (SBL1 and SBL2) were filtered, washed, and recrystallized with $C_2H_5OH$ and dried in desiccator over anhydrous $CaCl_2$ for three days.

**Synthesis of the mixed ligand complexes**

The mixed ligand metal(II) complexes were admixed with calculated amount of the SBL1, Metal salt and SBL2 in a 1:1:1 mole ratio following a reported literature method (Choudharya et al.,2020). To a 25mL of $C_2H_5OH$ solution, 1g of SBL1, (0.00301 mole), and 1.0697g of SBL2 (0.00301 mole) were with 0.added to 10mL of ethanoic solution of appropriate metal(II) salts (0.7377g, 0.60086g, and 0.8303g for Mn(II), Cu(II), and Fe(II) to give the ([Cu(L1)(L2)], [Fe(L1)(L2)$(H_2O)_2$]$H_2O$, and [Mn(L1)(L2)] respectively at 50$^0$C to 70$^0$C. The mixture was independently refluxed with constant stirring for 6 hours with the addition of a buffer solution (triethylamine) to maintain the pH of the solution. The precipitate formed was collected by gravity filtration, washed with $C_2H_5OH$ (10mL) and dried in desiccators over Calcium Chloride for 3days.

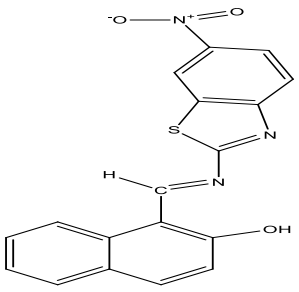


(a)

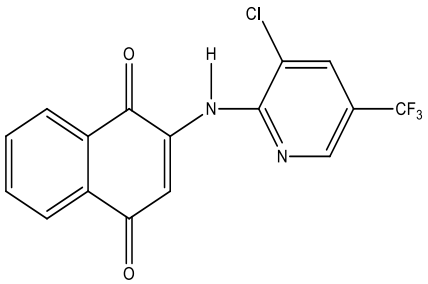


(b)


*Cite this article as*:
Wodi, T.C., & Festus, C. (2025). Multifaceted investigations of mixed-ligand metal (II) complexes: synthesis, characterization, DFT, and biological studies. *FNAS Journal of Scientific Innovations*, *6*(3), 1-14. https://doi.org/10.63561/fnas-jsi.v6i3.945

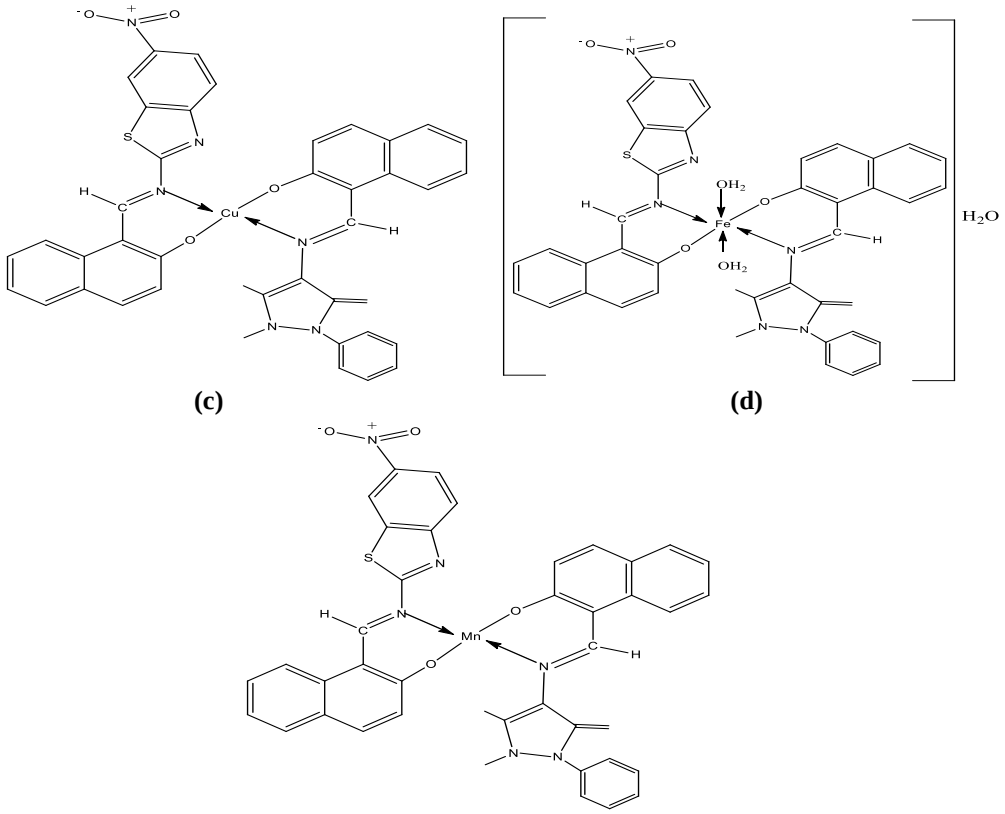


**Figure 1. Proposed Structures of the ligands and mixed ligand metal (II) complexes**; (a) SBL1(b) SBL2 (c) [Cu(L1)(L2)] (d) $[Fe(L1)(L2)(H_2O)_2]H_2O$ and (e) [Mn(L1)(L2)]

**Quantum chemical studies**

Quantum chemical calculations were performed using the Gaussian 09 software package (Rodrigues et al., 2022). DFT calculations with B3LYP/6-31G(d,p) level of theory was done according literature reported by Festus and Wodi (2021). The optimized structures are shown in figure 2. Global reactivity parameters and quantum chemical calculations were also employed. The optimized structure yields frontier molecular orbitals (HOMO and LUMO), enabling calculation of global reactivity (Akman, 2019).

**Global reactivity parameters**

DFT is widely used to calculate the electronic structure of molecules and solids including their energy levels, orbitals, and properties (Haque et al., 2018).

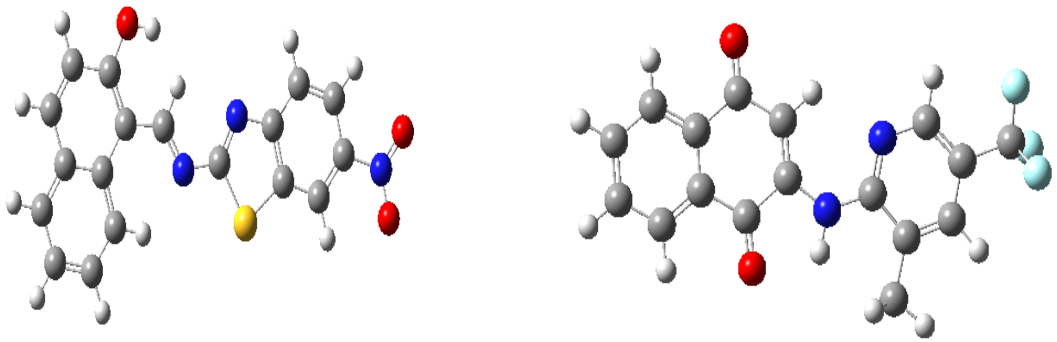

( a) (b)


*Cite this article as*:
Wodi, T.C., & Festus, C. (2025). Multifaceted investigations of mixed-ligand metal (II) complexes: synthesis, characterization, DFT, and biological studies. *FNAS Journal of Scientific Innovations*, *6*(3), 1-14. https://doi.org/10.63561/fnas-jsi.v6i3.945

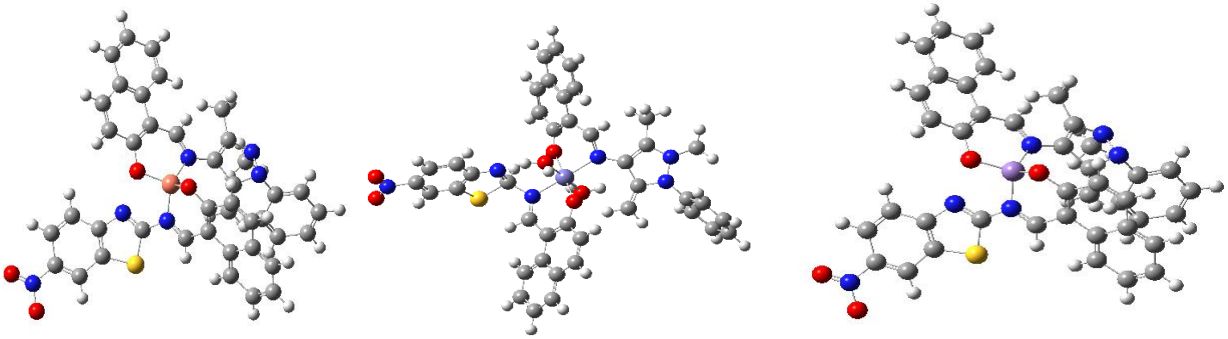

(c) (d) (e)

**Figure 2.** Optimized structure of (a) SBL1(b) SBL2 (c) [Cu(L1)(L2)] (d) $[Fe(L1)(L2)(H_2O)_2]H_2O$ and (e) [Mn(L1)(L2)] premeditated by B3LYP/6-31G (d, p**)**

## Results

### The physicochemical data of the ligands and the mixed ligands metal(II) complexes

The ligands displayed 278 to 280ºC;SBL1 and 208 – 216ºC;SBL2 melting point dissimilar from the initial chemicals. The mixed ligand complexes exhibited melting points greater than the ligands in the range: [Cu(L1)(L2)], 345-350ºC; $[Fe(L1)(L2)(H_2O)_2]H_2O$, 280-285ºC; and [Mn(L1)(L2)], 320-325ºC. The higher melting points of the complexes indicated a better stability (Inomata, 2024). [Cu(L1)(L2)] displayed the highest melting point which is attributed to its electronic configuration, Jahn-Teller distortion and the coordination geometry(Halcrow, 2013; Persson, 2002). Cu(II) has a $d_9$ electronic configuration which can lead to a more stable and symmetrical coordination geometry, resulting in stronger metal-ligand bonds and a higher crystal lattice energy(Shwan, 2022; Volkov et al., 2022). Cu(II) complexes often exhibit a jahn-Teller distortion, which can lead to a more rigid and stable structure (Halcrow, 2013). [Cu(L1)(L2)] adopted a square planar coordination geometry which can provide a more stable and rigid structure (Balewski et al., 2025). This rigidity can lead to higher melting point (Burak et al., 2024). The ligands displayed yellow shade while the mixed ligands metal(II) complexes displayed different shades of yellow. [Cu(L1)(L2)] had lemon yellow shade, [Mn(L1)(L2)]displayed black shade while $[Fe(L1)(L2)(H_2O)_2]H_2O$ displayed milk yellow shade. The display of different shades by the complexes maybe due their varied number of d-orbital electrons (Wang, 2024). Formation of metal complexes by a Schiff base may alter the electronic configuration of ligands thereby causing color changes of the compounds. Also, coordination of metal ions to the Schiff base can alter the ligand's electronic structure, leading to color changes (Arif et al., 2018). Other factors that influenced the color changes include solvent, pH, temperature and concentration (Arif et al., 2018; Ekennia et al., 2015). The mixed ligand metal(II) complexes showed different degrees of solubility in carbon-based solvents but were all insoluble in water and very soluble in dimethylformalde $(CH_3)_2NCHO$ and dimethylsulfoxide $(CH_3)_2SO$. Complex properties can lead to different level of solubility (Jagvir et al., 2019; Nisrme et al., 2021).

**Table 1: The physicochemical data of the ligands and their mixed ligands M(II) complexes**

| Compounds | Molecular formula | Colors | M.Pt(Cº) | Molecular weight |
|---|---|---|---|---|
| SBL1 | $C_{18}H_{11}O_3N_3S$ | Yellow | 278-280 | 349.29 |
| SBL2 | $C_{22}H_{18}O_2N_3$ | Yellow | 208– 216 | 355.39 |
| [Cu(L1)(L2)] | $CuC_{40}H_{29}O_5N_6S$ | Lemon Yellow | 345-350 | 767.24 |
| [Mn(L1)(L2)] | $MnC_{40}H_{29}O_5N_6S$ | Black | 320-325 | 757.63 |
| $[Fe(L1)(L2)(H_2O)_2]H_2O$ | $FeC_{40}H_{29}N_6O_5S.3H_20$ | Milk Yellow | 280-285 | 867.56 |

Key: SBL1= $C_{18}H_{11}O_3N_3S$, SBL2= $C_{22}H_{18}O_2N_3$, [Cu(L1)(L2)] = $CuC_{40}H_{29}O_5N_6S$, [Mn(L1)(L2)] = $MnC_{40}H_{29}O_5N_6S$, $[Fe(L1)(L2)(H_2O)_2]H_2O$ = $FeC_{40}H_{29}N_6O_5S$

### FT-IR spectra

Coordination of $Cu^{2+}$, $Fe^{2+}$ and $Mn^{2+}$ ions with functional groups of the mixed ligands SBL1 and SBL2 are established in Table (2) and Appendix (A-C). Assigning of the FTIR bands were made in match with the spectra of mixed ligands in literature on similar structures (Goni et al., 2022; Kpee et al., 2018, Mihsen & Shareef, 2018). The characteristics stretching vibration modes concerning ligands and the mixed ligand metal(II) complexes are described in Table 2. The


*Cite this article as*:
Wodi, T.C., & Festus, C. (2025). Multifaceted investigations of mixed-ligand metal (II) complexes: synthesis, characterization, DFT, and biological studies. *FNAS Journal of Scientific Innovations*, *6*(3), 1-14. https://doi.org/10.63561/fnas-jsi.v6i3.945

FTIR spectra of the ligands confirmed the formation of imine bond (-C=N-H) and the absence of carbony1 bond (C=O) with an absorption band noticed around 1633 and 1669 $cm^{-1}$ for SBL1 and SBL2 (Wodi & Festus 2021). This band was shifted and changed in complexes to lower and higher frequencies; 1625, 1641, and 1642$cm^{-1}$ for ([Cu(L1)(L2)], [Fe(L1)(L2)$(H_2O)_2$]$H_2O$, and [Mn(L1)(L2)] respectively because of coordination with metal ions through the nitrogen atom (Mihsen & Shareef, 2018; Sayed et al., 2020). The stretching vibration of C=C groups were observed in the spectra of SBL1 and SBL2 at 1589 and1625, which shifted to lower frequencies in the mixed ligand metal complexes; 1504, 1494, 1538$cm^{-1}$ for ([Cu(L1)(L2)], [Fe(L1)(L2)$(H_2O)_2$]$H_2O$, and [Mn(L1)(L2)] respectively. A sharp short intensity band presented at 1515 and 1567$cm^{-1}$ were assigned to the stretching vibration of N(C-N) in the ligands and were found at a lower wavelength in the mixed ligand metal complexes at 1290, 1016 and 1418$cm^{-1}$ for ([Cu(L1)(L2)], [Fe(L1)(L2)$(H_2O)_2$]$H_2O$, and [Mn(L1)(L2)] respectively (Sahar et al., 2021). A sharp short intensity band displayed at 823-827 $cm^{-1}$ was assigned to the stretching vibration of v(C-S) in the mixed ligand metal complexes (Fengtao et al., 2018). The broad bands observed around 3401 and 3389$cm^{-1}$ for SBL1 and SBL2 adjusted to a somewhat lesser wave-numbers amid 3332, 3263, and 3292 $cm^{-1}$ for ([Cu(L1)(L2)], [Fe(L1)(L2)$(H_2O)_2$]$H_2O$, and [Mn(L1)(L2)], respectively were assigned to v(O–H)($H_2O$). Results led to a suggestion for the presence of coordinated water molecules (Sayed et al., 2020). New bands at 520–747 $cm^{-1}$ and 480–562 $cm^{-1}$ indicated the coordination of the ligands to the central metal ion via nitrogen atom of imine group (M–N) and oxygen atom of the phenolic group (M–O) respectively (Wodi & Festus, 2021).

**Table 2: FTIR of the ligands and the mixed ligands metal(II) complexes**

| Compound | SBL1 | SBL2 | ([Cu(L1)(L2)] | [Mn(L1)(L2)] | [Fe(L1)(L2)$(H_2O)_2$]$H_2O$ |
|---|---|---|---|---|---|
| OH/$H_2O$ | 3401 | 3389 | 3332 | 3292 | 3263 |
| -C=N | 1633 | 1669 | 1625 | 1642 | 1641 |
| -C=C | 1589 | 1625 | 1504 | 1538 | 1494 |
| Cyclic C-N | 1515 | 1567 | 1290 | 1418 | 1016 |
| C=O/C-S | - | - | 1826 | 1823 | 1827 |
| C-C Stretch | | 990 | 1132 | - | - |
| CH rocking | | | - | - | 665 |
| C-O | 1122 | 1161 | 1048 | 1086 | - |
| $CH_3$ bend | | 1393 | 1337 | 1303 | 1075 |
| M-N | - | - | 747 | 602 | 520 |
| M-O | - | - | 562 | 482 | 480 |

**Electronic spectral measurement for the ligands (SBL1 and SBL2)**

Electronic spectra of the ligands are recorded in DMSO. The assignments for the electronic spectra are given in Table 3. SBL1 and SBL2 exhibit three/two bands in the UV region in the range of 32468-39379$cm^{-1}$ and 26850-29329$cm^{-1}$ which corresponds to π - π* and n - π* transitions respectively, according to their electronic spectra. The formation of metal ion complexes results in a shift of these bands to different wavelengths (bathochromic and hypochromic shifts) (Aderoju & Sherifah, 2015)

**Electronic spectral measurement of the mixed ligands metal(II) complexes**

The assignments of SBL1 and SBL2 UV/Visible spectra and its mixed ligands metal complexes were done by associating the observed values to earlier work on similar systems (Choudhary et al., 2020; Goni et al., 2022). The ligands showed three and four absorption bands at 39370, 32468, 29329$cm^{-1}$ in SBL1 and 38660, 33000[1], 26850, 18640$cm^{-1}$ in SBL2, respectively. The spectra of [Cu(L1)(L2)], [Mn(L1)(L2)] and [Fe(L1)(L2)$(H_2O)_2$]$H_2O$ presented several bands in the UV region in the range of 49504 – 20833$cm^{-1}$, which correspond to π - π* and n - π* transitions, respectively (Festus & Wodi, 2021). The visible spectrum of the [Cu(L1)(L2)] complex revealed two bands at 19762, and 12562$cm^{-1}$assigned to $^2B_1g \rightarrow {}^2A_1g$ transition and $^2B_1g \rightarrow {}^2Eg$ transition This suggests that the [Cu(L1)(L2)] complex has an Square Planar geometry ( Balewski et al., 2025; Diab et al., 2016; Lawal et al., 2017). The spectrum of [Mn(L1)(L2) displayed bands at 19193$cm^{-1}$ and 14662$cm^{-1}$ which were assigned to $^4A_2g \rightarrow {}^4T_2g$ and $^4A_2g \rightarrow {}^4T_2g$ transition. Considering the Mn(II) center and absorption pattern, the complex has a tetrahedral geometry ( Mahmoud et al.,2014). The spectrum of [Fe(L1)(L2)$(H_2O)_2$]$H_2O$ presented bands at 14771$cm^{-1}$, 14388, and 13210$cm^{-1}$ which were assigned to $^5T_{2g} \rightarrow {}^5E_g$, $^5T_{2g} \rightarrow {}^5T_{1g}$ and $^5T_{2g} \rightarrow {}^2T_{2g}$ transition ( Festus, 2021) conforming to an octahedral


*Cite this article as*:
Wodi, T.C., & Festus, C. (2025). Multifaceted investigations of mixed-ligand metal (II) complexes: synthesis, characterization, DFT, and biological studies. *FNAS Journal of Scientific Innovations*, *6*(3), 1-14. https://doi.org/10.63561/fnas-jsi.v6i3.945

assemblage. The presence of multiple d-d transitions at relatively low energies is consistent with an octahedral geometry (Onyenze et al., 2024).

**Table 3: Electronic studies of the mixed ligands metal(II) complexes**

| Compounds | Absorption Band ($cm^{-1}$) | Band Assessment | Geometry |
|---|---|---|---|
| SBL1 | 39370, 32468, 29329 | π-π* | |
| SBL2 | 38660, 33000 | π-π* | |
| | 26850, 18640 | n-π* | |
| [Cu(L1)(L2)] | 49504, 48006 | Charge transfer | |
| | 32258, 27322, 20833 | π-π* | |
| | 19762 | $^2B_{1g} \rightarrow {}^2A_{1g}$ $^2B_{1g} \rightarrow {}^2E_g$ | |
| | 12562 | | Square Planar |
| [Mn(L1)(L2)] | 29585, 28089, 27322, 24937 | n-π* | |
| | 19193 | $^4A_2g \rightarrow {}^4T_2g$ | |
| | 14662 | $^4A_2g \rightarrow {}^4T_1g$ | Tetrahedral |
| $[[Fe(L1)(L2)(H_2O)_2]H_2O$ | 31847, 28089, 27322 | π-π* | |
| | 14771 | $^5T_2g \rightarrow {}^5Eg$ | |
| | 14388 | $^5T_2g \rightarrow {}^5T_1g$ | Octahedral |
| | 13210 | $^5T_2g \rightarrow {}^5T_2g$ | |

**Anti-bacteria Action**

Antimicrobial actions of the ligands and the mixed ligand complexes, were determined against seven microbial strains using disc diffusion technique (Mahadev et al., 2016; Wodi & Festus, 2021) with diameter of the zones of growth inhibition presented in Table 4. Non-negative control used was streptomycin. The results indicated that all the tested complexes were active against the bacteria species. The result also indicated that the mixed ligands metal(II) complexes were more active against *Klebsiella pneumonia* than the parent ligands with [Mn(L1)(L2)] complex displaying a higher inhibition zone of 15.5mm compared to Streptomycin that displayed 11.5mm. The enhanced antibacterial activity of mixed metal(II) complexes was due to their increased lipid solubility, as explained by the overtone concept (Festus et al., 2023) and Tweedy's chelation theory (Wodi & Festus, 2021), which highlights the important of hydrophobicity in antimicrobial action. Upon coordination, the metal(II) ion's polarity is significantly reduced due to the overlap of the ligand's orbitals and the partial distribution of the metal ion's positive charge among the donor atoms. Furthermore, this process increases the delocalization of π electrons across the entire chelate ring, enhancing the lipophilicity of the complexes (Khan et al., 2017). As a result, the complexes can more easily penetrate lipid membranes, disrupting microbial metabolism. The enhanced antimicrobial activity of the metal(II) complexes can be attributed to the involvement of the metal ion in critical cellular processes.

**Table 4: Anti- bacterial actions of mixed ligands metal(II) complexes**

| **Complexes Compound** | ***Escherichia Coil*** | ***Stephylococusa ureus*** | ***StephylococusE pidermidis*** | ***Pseudomonas aeruginosa*** | ***Klebsiella pneumoniae*** | ***Bacillus subtilis*** | ***Proteus mirabilis*** |
|---|---|---|---|---|---|---|---|
| SBL1 | - | - | 6.0±0.0 | 2.0±0.0 | 6.5±0.5 | - | 8.0±0.0 |
| SBL2 | 7±1.0 | 9±1.0 | 14.5±0.5 | 6±1.0 | - | 7±1.0 | 3.5±0.5 |
| [Cu(L1)(L2)] | - | 6.5±0.5 | - | 12±0.0 | 9±1.0 | 8.5±0.5 | - |
| [Mn(L1)(L2)] | - | - | 5.5±0.5 | 6.5±0.5 | 15.5±0.5 | - | - |
| $[Fe(L1)(L2)(H_2O)_2]H_2O$ | - | - | 7±1.0 | | 13.5±0.5 | - | - |
| Streptomycin | 13±1.0 | 15±1.0 | 11.5±0.5 | 14.5±0.5 | 11.5±0.5 | 19.5±0.5 | 13.5±0.5 |


*Cite this article as*:
Wodi, T.C., & Festus, C. (2025). Multifaceted investigations of mixed-ligand metal (II) complexes: synthesis, characterization, DFT, and biological studies. *FNAS Journal of Scientific Innovations*, *6*(3), 1-14. https://doi.org/10.63561/fnas-jsi.v6i3.945

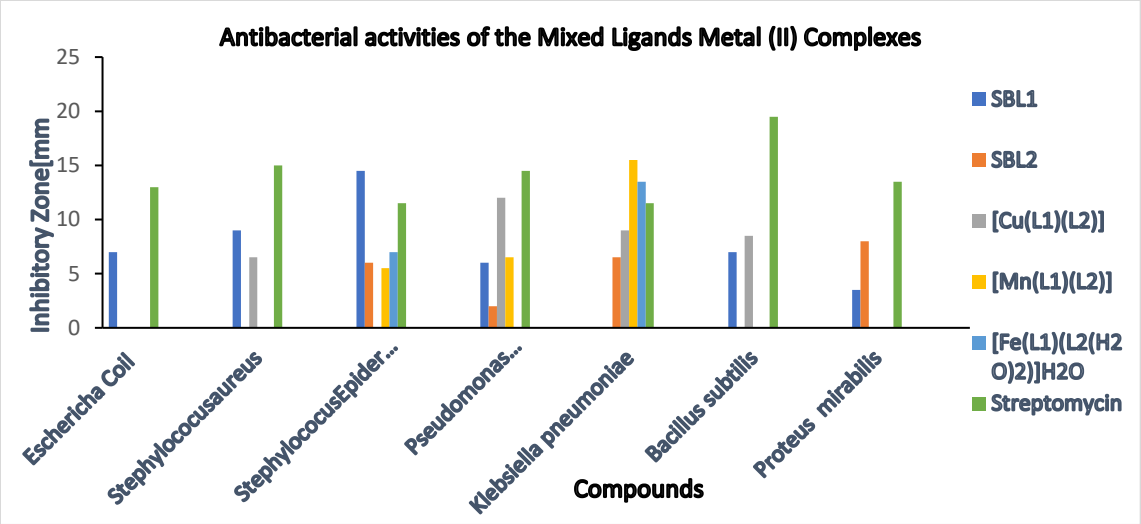


**Figure 3. Antibacterial activities of Mixed Ligands Metal (II) Complexes**

**Anti-fungal action**

The ligand and its mixed ligand metal(II) complexes were further subjected to anti-fugnal evaluations against three fungal strains; *Aspergillus niger*, *Aspergillus flavus*, *Fuserium sp.* Miconazole was adopted as positive control. The antifungal results (Table 5) showed that the ligands were active against the strains used. Aromatic chelators featuring C=N bonds and para-hydroxyl groups have been found to exhibit moderate antifungal activity against various fungal strains (Hayashi, 2016). All the ligands and mixed metal(II) complexes were active against the three fungi strains except ligand SBL2 and [Mn(L1)(L2)] which were inactive against *Aspergillus flavus,and Aspergillus niger*. SBL1 ligand displayed the highest inhibitory zones of 25.0 and 21.0mm against *Aspergillus niger* and *Aspergillus flavus* respectively. [Cu(L1)(L2)] complex also displayed the highest inhibitory zones of 17mm and 13mm against *Aspergillus niger* and *Aspergillus flavus*, all these values are higher than the positive control miconazole. The activities of the ligand and the complexes against the tested microbes were unexpectedly high and could be due to the presence of C=N- group and the hetero atoms in the ligand (Festus et al., 2019).

**Table 5: Anti fungal actions of mixed ligands metal(II) complexes**

| Compound | Aspergillus niger | Aspergillus flavus | Fusarium sp |
|---|---|---|---|
| SBL1 | 25±1.0 | 21.0±1.0 | 7.0±1.0 |
| SBL2 | - | - | 19±1.0 |
| [Cu(L1)(L2)] | 17±1.0 | 13±1.0 | 9.5±0.5 |
| [Mn(L1)(L2)] | - | - | - |
| $[Fe(L1)(L2)(H_2O)_2]H_2O$ | 6.5±0.5 | 3.5±0.5 | 14.5±0. |
| Miconazole | 13±1.0 | 11±1.0 | 8±0.0 |

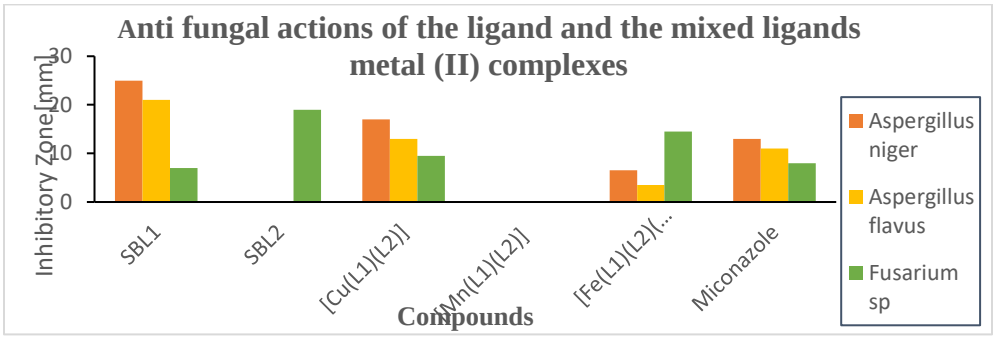


**Figure 4. Anti fungal actions of mixed ligands metal (II) complexes**


*Cite this article as*:
Wodi, T.C., & Festus, C. (2025). Multifaceted investigations of mixed-ligand metal (II) complexes: synthesis, characterization, DFT, and biological studies. *FNAS Journal of Scientific Innovations*, *6*(3), 1-14. https://doi.org/10.63561/fnas-jsi.v6i3.945

**Quantum chemistry study**

Figure 5 displays the optimized structures and frontier molecular orbitals (HOMO and LUMO) of the compounds, while Table 6 presents the corresponding quantum chemical descriptors. According to the frontier molecular orbital (FMO) theory, the interaction between the highest occupied molecular orbital (HOMO) and the lowest unoccupied molecular orbital (LUMO) facilitates electron transfer, influencing chemical reactivity (Yu et al., 2022). To understand a molecule's reactivity, it's crucial to examine its HOMO and LUMO energies. A molecule's ability to donate electrons is closely tied to its HOMO energy (EHOMO), which indicates its electron-donating capacity (Masnabadi et al., 2022). A high EHOMO value relative to ELUMO indicates a molecule's strong electron-donating capacity. Enabling it to readily transfer electrons to suitable acceptors with low-lying empty orbitals. This facilitates adsorption on metal surfaces, ultimately enhancing inhibition (Hadisaputra et al., 2022). In this work, higher EHOMO values (-6.10642, -6.20248, -7.613093, -6.87295 and -7.600677 for SBL1, SBL2, [Cu(L1)(L2)], $[Fe(L1)(L2)(H_2O)_2]H_2O$ and [Mn(L1)(L2)] suggest that the molecules can readily donate electrons to the metal surface (Ayuba et al., 2024). Furthermore, smaller energy gaps ($\Delta E = E$lumo–$E$Homo) facilitate better inhibition efficiency, as less energy is required to remove an electron from the highest occupied orbital, enhancing the molecule's reactivity (Festus et al., 2022; Abd El-Lateef et al., 2020). The studied molecules SBL1, SBL2, [Cu(L1)(L2)], $[Fe(L1)(L2)(H_2O)_2]H_2O$ and [Mn(L1)(L2)] exhibited relatively small energy gaps (3.21035eV, 3.153215eV, 0.224218eV, 0.46449eV and 1.713578eV respectively) and small energy gaps indicates greater softness compared to similar molecules in other studies (Udhayakala & Rajendiran, 2015; Sharma et al., 2016). A smaller energy gap between EHOMO and ELUMO indicates easier electron transfer, facilitating increased chemical reactivity and enhanced adsorption (Abd El-Lateef et al., 2020). The mixed ligand metal(II) complexes ([Cu(L1)(L2)], $[Fe(L1)(L2)(H_2O)_2]H_2O$ and [Mn(L1)(L2)] exhibited higher chemical reactivity and adsorption than the ligands (SBL1, & SBL2) due to their smaller energy gaps.

**Table 6. Quantum chemical variables**

| **Parameters /Inhibitors** | SBL1 | SBL2 | [Cu(L1)(L2)] | $[Fe(L1)(L2)(H_2O)_2]$ $H_2O$ | [Mn(L1)(L2)] |
|---|---|---|---|---|---|
| Homo | -6.10642 | -6.20248 | -7.61309 | -6.8730 | -7.60068 |
| Lumo | -2.89607 | -3.04926 | -7.38888 | -6.4085 | -5.88710 |
| Gap | 3.21035 | 3.153215 | 0.224218 | 0.46449 | 1.713578 |
| Ionization .P | 6.10642 | 6.20248 | 7.613093 | 6.87295 | 7.600677 |
| *A* | 2.89607 | 3.04926 | 7.388875 | 6.40846 | 5.887099 |
| X | 4.50125 | 4.62587 | 7.500984 | 6.64071 | 6.74389 |
| Chpot | -4.50125 | -4.62587 | -7.50098 | -6.6407 | -6.74389 |
| Hard | 1.605175 | 1.57661 | 0.112109 | 0.23225 | 0.856789 |
| Soft | 0.622985 | 0.63427 | 8.919805 | 4.30580 | 1.167149 |
| Ω | 1.402106 | 1.46703 | 66.90796 | 28.5929 | 3.935561 |
| ΔE | 3.21035 | 3.15322 | 0.224218 | 0.46449 | 1.713578 |
| μ | -4.50125 | -4.62587 | -7.500984 | -6.64071 | -6.74389 |
| μ (D) | 7.51259 | 4.561784 | 10.24189 | 20.7119 | 7.74657 |

Chemical potential is an electronic descriptor that predicts a material's reactivity (Oyebamiji & Adeleke, 2018) based on the uneven distribution of charges among its atoms. There's an insignificant correlation between chemical potential values and inhibition efficiencies. Hardness and softness (η and *S*) indicators assess molecular reactivity and strength. Electron affinity measures a molecule's tendency to accept electrons, while ionization potential measures its tendency to donate electrons (Gouda, et al., 2022; Odozi et al., 2020). The molecules studied SBL1, SBL2, [Cu(L1)(L2)], $[Fe(L1)(L2)(H_2O)_2]H_2O$ and [Mn(L1)(L2)] exhibit high ionization potential (I) and electron affinity (A) values, indicating their ability to both donate and accept electrons. The inhibitor's electronegativity values ($\chi$) indicate their capacity to donate or accept electron from the metal surface, with most showing a high tendency to donate elections (Palaniappan et al., 2020). High electronegativity values indicate the inhibitor's strong ability to attract electrons from the metal surface, forming a robust bond (Abd El-Lateef Abd et al., 2020). Electrophilicity (ω) measures a molecule's reactivity by combining information on its hardness and chemical potential. High electrophilicity values indicate


*Cite this article as*:
Wodi, T.C., & Festus, C. (2025). Multifaceted investigations of mixed-ligand metal (II) complexes: synthesis, characterization, DFT, and biological studies. *FNAS Journal of Scientific Innovations*, *6*(3), 1-14. https://doi.org/10.63561/fnas-jsi.v6i3.945

strong electorn-accepting ability (electrophilic character) while low electrophilicity values suggest electron-donating tendency (nucleophilic character). This implies a correlation between electrophilicity values and a molecule's reactivity profile (Diki et al., 2021; Gouda et al., 2022). In this work, high electrophilicity values of 66.90796eV & 28.5929eV for [Cu(L1)(L2)] and [Fe(L1)(L2)$(H_2O)_2$]$H_2O$ respectively designates that they are good electrophile which specifies strong electron accepting tendency while [Mn(L1)(L2)] showed moderate electrophilicity of3.935561eVindicating moderate electron acceptor. SBL1 and SBL2 exhibits low electrophilicity values of 1.402106eV and 1.46703eV suggesting electron-donating tendency (nucleophile).

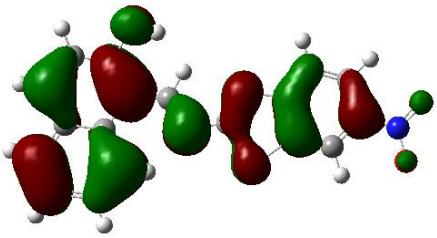

(ai) SBL1 HOMO

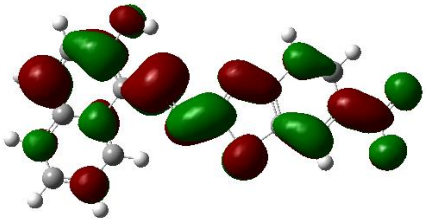

(aii) SBL1 LUMO

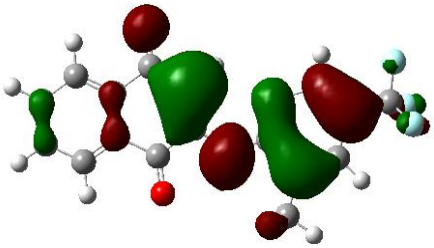

(bi) SBL2 HOMO

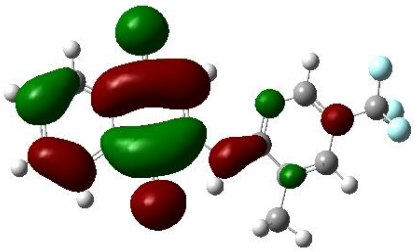

(bii) SBL12 LUMO

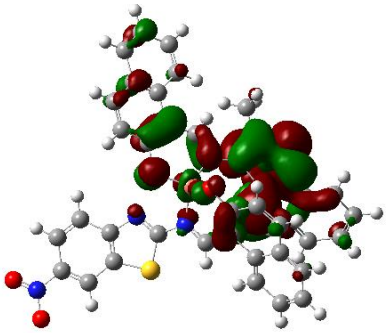

(ci) [Cu(L1)(L2)] HOMO

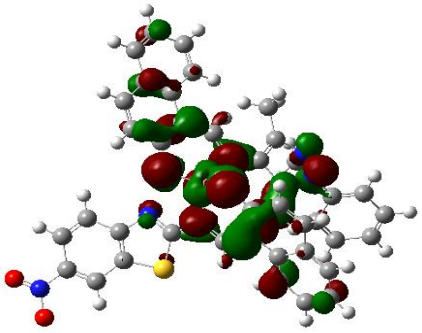

(cii) [Cu(L1)(L2)] LUMO

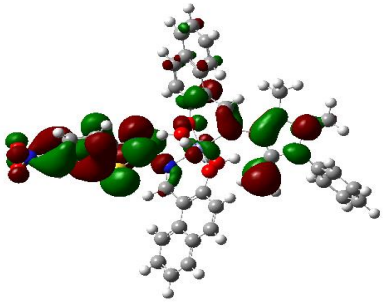

(di) [Fe(L1)(L2)$(H_2O)_2$]$H_2O$ Homo

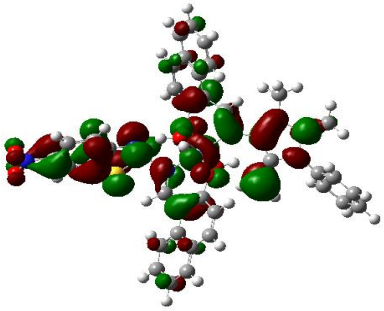

(dii) [Fe(L1)(L2)$(H_2O)_2$]$H_2O$ Lumo


*Cite this article as*:
Wodi, T.C., & Festus, C. (2025). Multifaceted investigations of mixed-ligand metal (II) complexes: synthesis, characterization, DFT, and biological studies. *FNAS Journal of Scientific Innovations*, *6*(3), 1-14. https://doi.org/10.63561/fnas-jsi.v6i3.945

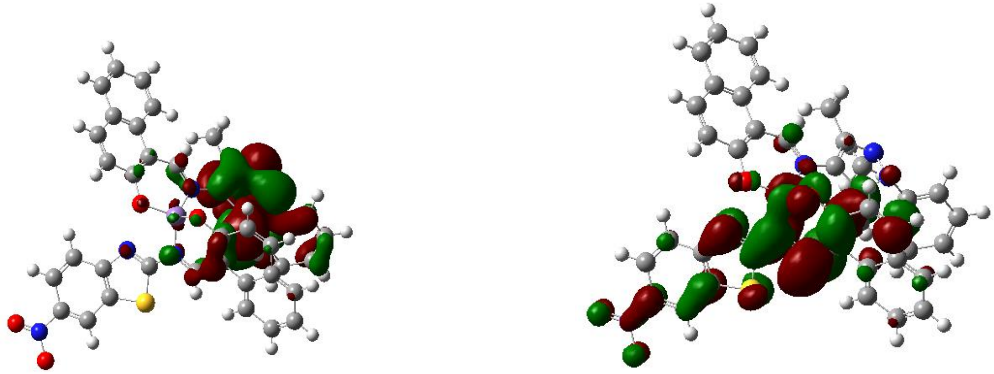

(ei) [Mn(L1)(L2)] Homo (eii) [Mn(L1)(L2)] Lumo

**Figure 5. HOMO and LUMO diagrams of (a) SBL1 (b) SBL2(c) [Cu(L1)(L2)] (d) [Fe(L1)(L2)($H_2O$)$_2$]$H_2O$ and (e) [Mn(L1)(L2)] by B3LYP/6-31G (d, p).**

## Conclusion

Two ligands; SBL1 = $C_{18}H_{11}O_3N_3S$ and SBL2=$C_{22}H_{18}O_2N_3$ plus three mixed ligands metal(II) complexes; [Mn(L1)(L2)] = $MnC_{40}H_{29}O_5N_6S$, [Fe(L1)(L2)($H_2O$)$_2$]$H_2O$ =$FeC_{40}H_{29}N_6O_5S$, and [Cu(L1)(L2)] = $CuC_{40}H_{29}O_5N_6S$ complexes were integrated by reacting metal salts with a mixture of two different ligands in a specific molar ratio: ligand1, M(II) salt and Ligand2 (1:1:1 ). The compounds were characterized by different spectroscopic methods which confirmed their formation. A Square, tetrahedral and octahedral geometry were assigned to Cu, Mn and Fe complexes respectively. The ligands and the mixed ligand metal (II) complexes had countless shades of colour distinct from the starting reagents. The infrared spectral of the ligands confirmed the formation of imine bond (-C=N-H) and the absence of carbony1 bond (C=O) with an absorption band noticed around 1633 and 1669 $cm^{-1}$ for SBL1 and SBL2. The imine bond was also existent in the mixed ligand metal complexes at wavenumbers amid, 1625, 1641, and1642$cm^{-1}$ for [Cu(L1)(L2)], [Fe(L1)(L2)($H_2O$)$_2$]$H_2O$, and [Mn(L1)(L2)] complexes respectively showing involvement of the imine nitrogen atom in coordination with the M(II) ions. From the antimicrobial result, SBL2 displayed highest inhibitory zone of 14.5mm against *Stephylococus epidermidis* which is higher than the positive control streptomycin, all the complexes showed active inhibitory zones against *Klebsiella pneumonia* with [Mn(L1)(L2)] and [Fe(L1)(L2)($H_2O$)$_2$]$H_2O$ displaying higher inhibition zone of 15.5mm and 13.5mm respectively compared to Streptomycin that displayed 11.5mmn inhibitory zone. The anti-fungiform study designated that the ligands and the Mixed ligand metal(II) complexes are highly active against *Aspergillusm flavus*, *fuserium sp.* and *Aspergillus niger*. SBL2 ligand displayed the highest inhibitory zones of 25.0 and 21.0mm against *Aspergillus niger* and *Aspergillus flavus* respectively. [Cu(L1)(L2)] complex also displayed the highest inhibitory zones of 17mm and 13mm against *Aspergillus niger* and *Aspergillus flavus*, which are higher than the positive control miconazole. The electronic, structural and spectroscopic properties of the complexes were further discussed using density functional theory. The result designated that the ligand is a soft molecule because it has a high tendency of bioavailability and can be a better agent against bacteria. The mixed ligand metal(II) also showed a high electrophilic values which indicates strong electron acceptor.

## Refrences

Abdullahi, M. Muhammed, S. & Sani, S. (2018). Synthesis and Characterization of Some Mixed Ligands Adducts of Benzoylacetone and Salicylaldehyde. *Bayero Journal of Pure and Applied Sciences*, 11(1), 168-173.

Abd El-Lateef, H.M., Shalabi, K., & Tantawy, A.H.(2020). Corrosion inhibition of carbon steel in hydrochloric acid solution using newly synthesized urea-based cationic flfluorosurfactants: Experimental and computational investigations. *New Journal in Chemistry, 44*, 17791–17814

Aderoju, A. O. & Sherifah, M. W. (2015). Synthesis, Characterization and Antimicrobial Activity of some mixed Trimethoprim-sulfamethoxazole metal complexes. *World Applied Science Journal*, 33(20), 336-342.

Akman, F. (2019). A density functional theory study based on monolignols: molecular structure, HOMO-LUMO analysis, molecular electrostatic potential. *Cellulose Chemistry and Technology*, 53(3-5), 243-250. Doi.org/10.35812/celluloseChemTechnol.2019.53.24



*Cite this article as*:
Wodi, T.C., & Festus, C. (2025). Multifaceted investigations of mixed-ligand metal (II) complexes: synthesis, characterization, DFT, and biological studies. *FNAS Journal of Scientific Innovations*, *6*(3), 1-14. https://doi.org/10.63561/fnas-jsi.v6i3.945

Arif, A.R., Nayab, P.S., Ansari, I.A., Shahid, M., Irfan, M., Alam, S., & Abid, M. (2018).Synthesis, molecular docking and DNA binding studies of phthalimide based copper(II) complex: in vitro antibacterial, hemolytic and antioxidant assessment. *Journal of Molecular Structure*. 1160, 142-153.

Ayuba, A. M., Lorhuna, F., & Nyijime, A.T. (2024). Corrosion inhibition activities of Acridine Derivatives on Aluminium using Fukui function and Molecular dynamic. *Progress in Chemical and Biochemical Research*, 7(4), 453-471.

Balewsi, L., Stepniak, I. I., Gdaniec, M., Turecka, K., Fering, A., Ordyszewska, A., & Kornicka, A. ( 2025). Synthesis, structure, and stability of copper(II) complexes containing imidazoline-phthalazine ligands with potential anticancer activity. *Pharmaceuticals*, 18(3), 375.

Burak, K., Hakan, F.O., Nirmalendu, B., & Faith, S. (2024). Effects of geometrical configurations on melting and solidification processes in phase change materials. *Applied Thermal Engineering*, 258(C), 124726. Doi.org/10.1016/j.appithermaleng.2024.124726

Choudharya A., Sharmaa R., & Nagara M.(2020). Synthesis, characterization and antimicrobial activities of mixed of Co(II) and Cu(II) of N, O/S ligands and amino acids. *International Journal of Pharmacy and Pharmacology*, 9(9), 001-016

Diab, M.A., El-Sonbati, A.Z., El-Bindary, A.A., Morgan, S.M., & El-Kader, M.A. (2016). Geometrical Structures, molecular docking, spectroscopic characterization of mixed ligand and Schiff base metal complexes. *Journal of Molecular Liquids*, 218, 571-585.

Diki, N.Y.S., Coulibaly, N.H., Kambiré, O. and Trokourey, A.(2021) Experimental and Theoretical Investigations on Copper Corrosion Inhibition by Cefixime Drug in 1M HNO3 Solution. *Journal of Materials Science and Chemical Engineering*, 9, 11-28.

Ekennia, A.C., Onwudiwe, D.C., Ume, C., & Ebonso, E. (2015). Mixed Ligand Complexes Of N-Methyl-N-Phenyl Dithiocarbanate: Synthesis, Characterization, Antifungal Activity and Solvent Extraction Studies of the Ligand. *Bioinorganic Chemistry and Applications*, 1, 913424

Farhi, S.A., Moataz, M., Khlood, A.M., & Nashwa, M. E. (2023). Synthesis and Characterization of New Mixed ligand Complexes; Density Function Theory, Hirshfeld and in silico Assays strengthen the Bioactivity performed in Vitro. *ACS Omega*, 8(4), 4220- 4233.

Fengtao, Y., Zhiqiang, W., Shicong, Z., Haonan, Y., Kangyi, K., Xueqing, G., Jianili, H., & He, T., (2018). Molecular Engineering of Donor-Acceptor Conjugated Polymer/g $C_3N_4$ Hetero structures for significantly Enhanced Hydrogen Evolution Under Visible- Light Irradiation. *Advanced Functional Materials*, 28, 1804512.

Festus, C., & Okocha, O. (2017). Behaviour of N-(2-hydroxybenzylidene)pyrazine-2-carboxamide in complexation towards Fe(II), Co(II), Ni(II) and Cu(II) ions: synthesis, spectral characterization, magnetic and antimicrobial properties. *International Journal of Chemical, Pharmaceutical & Technology*, 2(4), 143-153.

Festus, C., Don-Lawson, C. D. & Ima-Bright, N. (2019). Synthesis involving asymmetric pyrazine-Schiff base with Co2+,Ni2+ and Cu2+ ions: Spectral, and magnetic characterizations, and antibacterial studies. *International Journal of Research and Innovation in Applied Science*, 4(4)

Festus, C., Chizoba, I. E., & Obinna, O. (2023). Synthesis, characterization, DFT and biological studies of Fe(II), Cu(II), and Zn(II) complexes of keto-imine chelators. *Inorganica Chimica Acta, 545*(2023), 121255.

Festus, C**.,** Odozi, W. N., Mchihim, M. M., & Olatunde, M. A. (2022). Synthesis, spectroscopic, density functional theory and corrosion inhibitive studies of *N*-(1,4-dihydro-1,4-dioxonapthalene-3-yl)pyrazine-2-carboxamide chelator-ligand. *Global Journal of Pure & Applied Sciences, 28*, 39-50.

Festus, C. & Wodi, C. T. (2021). Corrosion Inhibition; and Antimicrobial Studies of Bivalent Complexes of 1-(((5-ethoxybenzo[d]thiazol-2-yl)Imino)methyl)naphthalene-2-ol Chelator: Design, Synthesis, and Experimental Characterizations. *Direct Research Journal of Chemistry and Materials Science*, 8(2021); 31-43.

Fran, Z. K., & Metzler-Nolte, N. (2019). Introduction to metals in medicine. *Chemical Research Journals*, 119, 727 -729.

Goni, M., Ndahi, P.N., Yesufu, P.H., Kyari, S.F., & Usman, Y.F. (2022). Synthesis, characterization and antioxidant activity of mixed ligand complexes of Mn, Co, Ni, Cu, and Zn ions with Nicotinic acid and phenylalanine. *Arid Zone Journal of Basic and Applied Research*, 1(3), 1-16.

Gouda, M., Khalaf, M., Shalabi, K., Al-Omair, M., & Abd El-lateef, H. M. (2022). Synthesis and characterization of Zn organic frameworks containing chitosan a low cost inhibitor for sulphuric acid induced steel corrosion: *practical and computational exploration. Polymer*, 14,228.

Haque, J., Verma, C., Srivastava, V., Quraishi, M., & Ebenso, E. (2018). Experimental and quantum chemical studies of functionalized tetrahydropyridines as corrosion inhibitors for mild steel in 1 M hydrochloric acid. *Results In Physics*, *9*, 1481-1493.

Hadisapitra, S., Purwoko, A.A., Hakim, A., Prasetyo, N., & Hamdiani, S. (2022). Corrosion inhibition properties of Phenyl phthalimide derivatives against carbon steel in the acidic medium: DFT, MP2, and Monte Carlo simulation studies. *ACS Omega*, 7(37), 33054-33066.

Halcrow, M. (2013). Jahn-Teller distortions in transition metal compounds, and their importance in functional molecular and inorganic materials. *Chemical Society Reviews*, 42(4), 1784-1795 Doi:10.1039/c2cs35253b

Hema, M.K, Karthik C.S, Rajabathar J.R, Hamad A.A, Hassan A, Selvaraj A., Dafellah M. A, Lokanath N.K. (2024). A new mixed-ligand mononuclearCo(II) derived from 4,4,4 derived from 4,4,4-trifluoro-1-phenylbutane-1,3-dione and 1,10-phenanthradine: Synthesis, Structural Elucidation and Quantum-computational studies. *Journal of molecular structure*, 1299, 137169.

Inomata, T. (2024). Stability of Metal Complexes and Ligand Substitution Reactions. *Chemistry Fundamentals Series*, 148-166.

Jagvir, S., Srivastav N., Netrapal, S., & Anradha, S. (2019). Stability Constants of Metal Complexes in Solution. *Chapter Metrics Overview*. Doi:10.57721/intechopen.90183

Jean-Pierre, L. (2019). Mixed-Valent compounds and their properties – recent developments. *European Journal of Inorganic Chemistry*, 2020(4), 329-341.

Khan, S. A., Shahab, N..A., Shahnawaz, B. A., & Kareem, N. A. (2017). Synthesis, characterization and antimicrobial study of polymeric transition metal complexes of Mn(II), Co(II), Ni(II), Cu(II) and Zn(II). *Microbial Pathogen*, 110, 414–425,

Kpee, F., Ukachukwu, C. V., & Festus, C. (2018). Synthesis, characterization and extractive potentials of aminopyrimidine Schiff base ligands on divalent metal ions. *Nigerian Research Journal of Chemical Sciences*, *4*(2), 193-203

Lawal, M. O., Bamigboye, J. A., Nnabuike, M. O., Ayinla, G. G., Rajee, S. O., Babamale, A. O., & Ajibola, A. A. (2017). Mixed Metal Complexes of Isoniazid, and Ascorbic Acid: Chelation, Characterization and Antimicrobial Activities. *Nigeria Journal of Chemical Research*, 22(1), 20-28.

Masnabadi, N., Thaiji, M.O., Mahmoodi, Z., Soldatov, A.V., & Ali, G.A. (2022). Structural, Electronic, reactivity, and conformational features of 2, 5, 5-trimethyl-1, 3, 2-diheterophosphinane-2-sulfide, and its derivatives: DFT, MEP, and NBO calculations. *Molecules*, 27(13), 4011.

Meena R, Meenam P, Kumari, A., Sharma, N., & Fahmi, N. (2022). Schiff bases and their metal complexes: synthesis, structural, characteristics and applications. *Chapter metrics overview*. Doi:10.5772/intechopen.108396

Mihsen, H.H., & Shareef,, K.N. (2018). Synthesis, characterization of mixed ligand complexes containing 2,2-bipyridine and 3-aminopropytriethoxysilane. *Journal of Physics: Conference Series*, 1032,012066.

Nisrine, J., Rosario, O., Stewart, G., Charles, C., & Roland, W. (2021). The Effect of Temperature and Pressure on Protein-Ligand Binding in the Presence of Mars-Relevant Salts. *Bilogy (Basel)*, 10(7), 687. Doi:10.3390/biology10070687.

Onyenze, U., Otuokere, I.E., & Enogbe, J.E. (2024). Synthesis, characterization and Antibacteria screening of Fe(II) mixed ligand complex of Ofloxacin with Ascorbic Acid. *European Journal of Scientific Research and Reviews*, 1(2), 112-118.

Oyebamiji, A.K., & Adeleke, B.B. (2018). Quantum chemical studies on inhibition activities of 2,3-dihydroxypropyl-sulfanyl derivative on carbon steel in acidic media. *International Journal of Corrosion. Scale Inhib.7*, 498–508.

Palaniappan, N., Cole, I.S., & Kuznetsov, A.E. (2020). Experimental and computational studies of graphene oxide covalently functionalized by octylamine: Electrochemical stability, hydrogen evolution, and corrosion inhibition of the AZ13 Mg alloy in 3.5% NaCl. *Royal Society of Chemistry Advances, 10*, 11426–11434.

Persson, I., Persson, P., Sandstrom, M., & Ullstrom, A. (2002). Structure of Jahn-Teller distorted solvated copper(II) ions in solution, and in solids with apparently regular octahedral coordination geometry. *Journal of the Chemical Society, Dalton Transactions*, 7, 1256-1265. Doi.org/10.1039/B200698G

Rodrigues, D.J., Santos, L.M., Melo, A., & Lima, C.F. (2022). Theoretical study on the Diels-Alder reactions of fullerenes: Analysis of isomerism, aromaticity, and solvation. *Organics*, 3(4), 364-379. Doi.org/10.3390/org3040025

Sayed, S. S., Dawood, S., Ibrahim, K., Sajjad, A. A., & Atiq, U. R. (2020). Synthesis, Antioxidant Activities of Schiff base and their complexes: An updated review. *Biointerface Research in Applied Chemistry*. 1016, 6936-6963.

Sahar, F. A., Jummbad, H. T., & Emad, T. A., (2021). Synthesis and Chariterization of New Schiff Bases and their 1,3-Oxazepines Derived from Phthalic Anhydride. *Systematic Review Pharmaceutical*. 12(2), 260-265

Sharma, V., Arora, E. K. & Cardoza, S. (2016). Syntheses, Antioxidant, antibiotic and DFT study on acoumarin based salen-type Schiff base and its copper complex. *Journal chemical papers*. https://doi.org/10.1515/chempap-2016-0083.70(11), 1493-1502

Shwan, H.Y. (2022). John-Teller distortion in octahedral hexaquacopper(II) transition for S=1/2, d9 metal complex. *Journal of university of Balbylon for Pure and Applied Sciences*, 30(1). Doi.1029196/jubpas.v30i1.4064

Udhayakala, P. & Rajendiran, T.V. (2015) A Theoretical Evaluation on Benzothiazole Derivatives as Corrosion Inhibitors on Mild Steel. *Der Pharma Chemica*, **7**, 92-99

Wodi, T. C., Festus, C., & Nlemonwu, E. (2022). Anti-corrosion potentials of naphtha-quinone/naphtha-aldehyde Schiff bases for mild steel in HCl medium: Synthesis, characterization and DFT studies. *Journal of Chemical Society of Nigeria, 47*(5), 1075-1098

Yu, J., Neil, Q. S., & Yang, W., (2022). Describing chemical reactivity with frontier molecular orbitals. *American Chemical Society*, 2, 6, 1383- 1394.

## Appendix

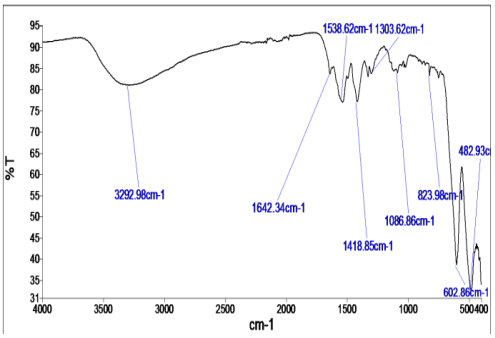


**A:** Infrared Spectrum of [Mn(L1)(L2)]

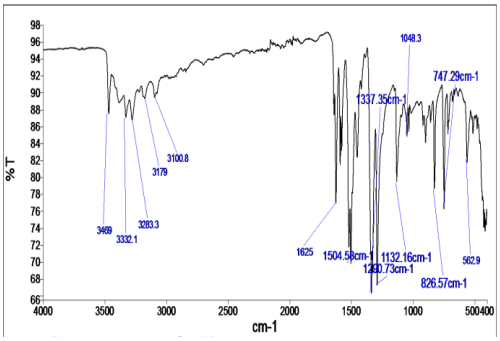


B: Infrared Spectrum of [Cu(L1)(L2)]

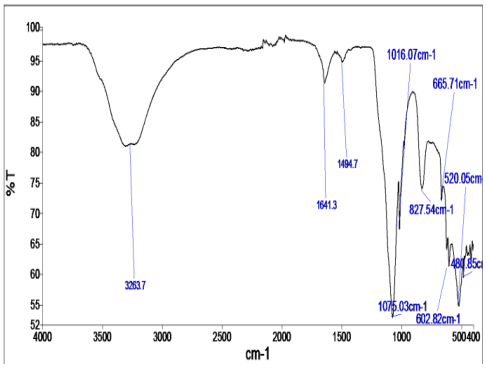


**C:** Infrared Spectrum of $[Fe(L1)(L2)(H_2O)_2]H_2O$

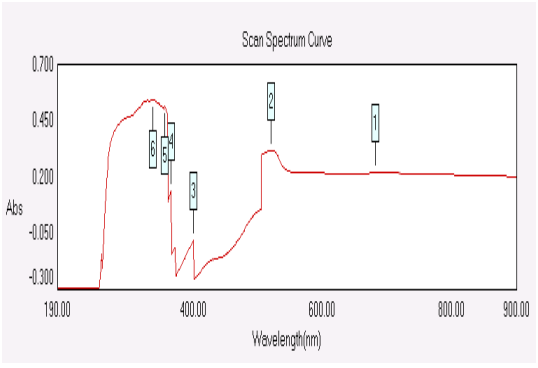


D: Electronic Spectra Of $[Mn(L1)(L2)]2H_2O$



*Cite this article as*:
Wodi, T.C., & Festus, C. (2025). Multifaceted investigations of mixed-ligand metal (II) complexes: synthesis, characterization, DFT, and biological studies. *FNAS Journal of Scientific Innovations*, *6*(3), 1-14. https://doi.org/10.63561/fnas-jsi.v6i3.945

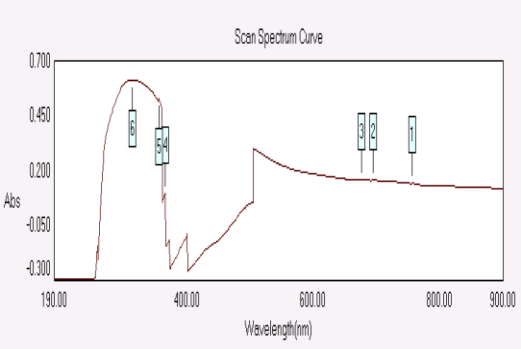


**E:** Electronic Spectra of $[Fe(L1)(L2)(H_2O)_2]H_2O$

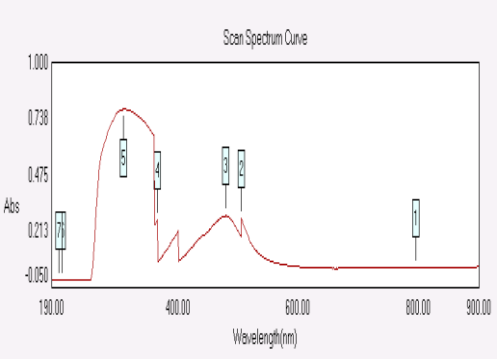


F: Electronic Spectra of $[Cu(L1)(L2)]$

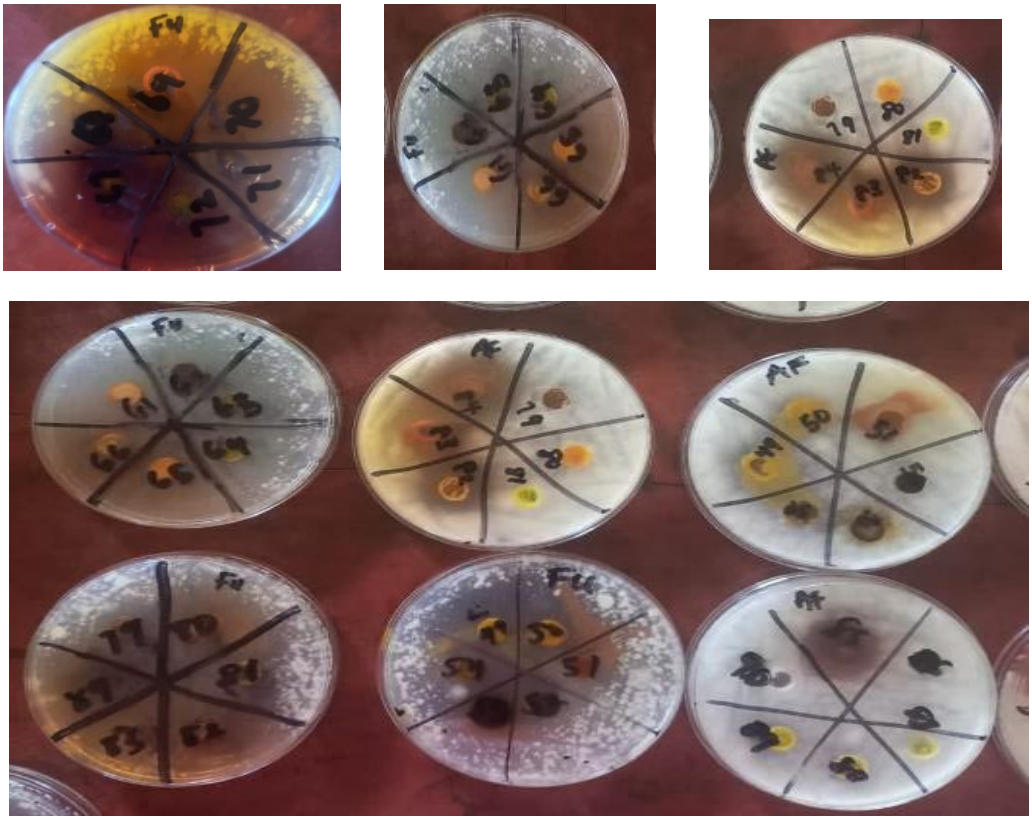

**G: Bacterial and Fungal Activities of The Mixed Ligand Metal(II) Complexes**


*Cite this article as*:
Wodi, T.C., & Festus, C. (2025). Multifaceted investigations of mixed-ligand metal (II) complexes: synthesis, characterization, DFT, and biological studies. *FNAS Journal of Scientific Innovations*, *6*(3), 1-14. https://doi.org/10.63561/fnas-jsi.v6i3.945